Children's Mercy Kansas City

SHARE @ Children's Mercy

Manuscripts, Articles, Book Chapters and Other Papers

1-2022

Next-Generation Sequencing of Minimal Residual Disease for Predicting Relapse after Tisagenlecleucel in Children and Young Adults with Acute Lymphoblastic Leukemia.

Michael A. Pulsipher

Xia Han

Shannon L. Maude

Theodore W. Laetsch

Muna Qayed

See next page for additional authors

Let us know how access to this publication benefits you

Follow this and additional works at: https://scholarlyexchange.childrensmercy.org/papers

 Part of the Oncology Commons, and the Pediatrics Commons

Recommended Citation

Pulsipher MA, Han X, Maude SL, et al. Next-Generation Sequencing of Minimal Residual Disease for Predicting Relapse after Tisagenlecleucel in Children and Young Adults with Acute Lymphoblastic Leukemia. Blood Cancer Discov. 2022;3(1):66-81. doi:10.1158/2643-3230.BCD-21-0095

This Article is brought to you for free and open access by SHARE @ Children's Mercy. It has been accepted for inclusion in Manuscripts, Articles, Book Chapters and Other Papers by an authorized administrator of SHARE @ Children's Mercy. For more information, please contact hlsteel@cmh.edu.

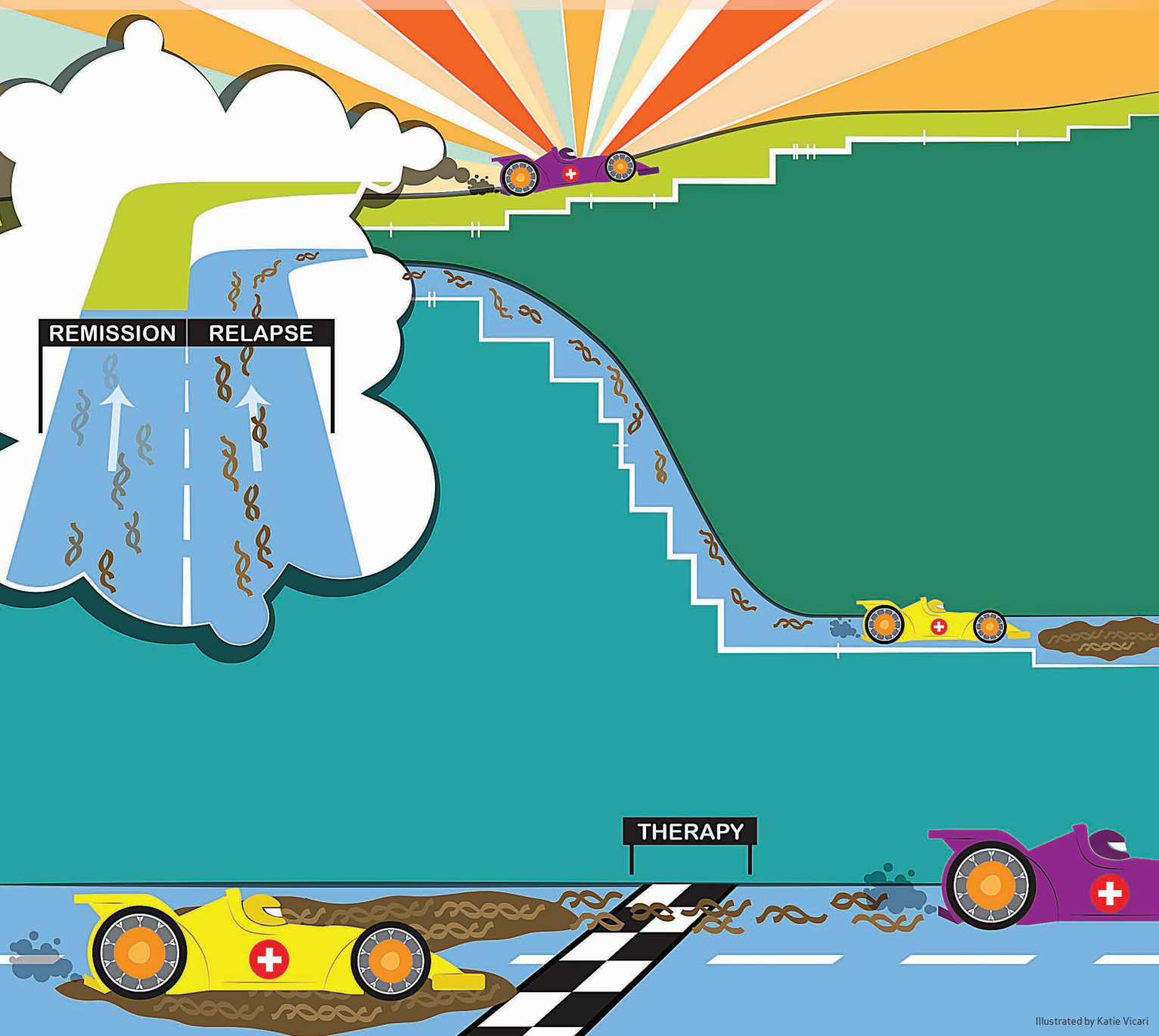
Creator(s)
Michael A. Pulsipher, Xia Han, Shannon L. Maude, Theodore W. Laetsch, Muna Qayed, Susana Rives, Michael W. Boyer, Hidefumi Hiramatsu, Gregory A. Yanik, Tim Driscoll, Douglas Myers, Peter Bader, Andre Baruchel, Jochen Buechner, Heather E. Stefanski, Creton Kalfoglou, Kevin Nguyen, Edward R. Waldron, Karen Thudium Mueller, Harald J. Maier, Gabor Kari, and Stephan A. Grupp

This article is available at SHARE @ Children's Mercy: https://scholarlyexchange.childrensmercy.org/papers/4177

RESEARCH ARTICLE

Next-Generation Sequencing of Minimal Residual Disease for Predicting Relapse after Tisagenlecleucel in Children and Young Adults with Acute Lymphoblastic Leukemia

Michael A. Pulsipher[1], Xia Han[2], Shannon L. Maude[3,4], Theodore W. Laetsch[3,4,5], Muna Qayed[6,7], Susana Rives[8], Michael W. Boyer[9], Hidefumi Hiramatsu[10], Gregory A. Yanik[11], Tim Driscoll[12], G. Doug Myers[13], Peter Bader[14], Andre Baruchel[15,16], Jochen Buechner[17], Heather E. Stefanski[18], Creton Kalfoglou[2], Kevin Nguyen[2], Edward R. Waldron[2], Karen Thudium Mueller[2], Harald J. Maier[19], Gabor Kari[19], and Stephan A. Grupp[3,4]



Illustrated by Katie Vicari

ABSTRACT We assessed minimal residual disease (MRD) detection and B-cell aplasia after tisagenlecleucel therapy for acute lymphoblastic leukemia (ALL) to define biomarkers predictive of relapse ($N = 143$). Next-generation sequencing (NGS) MRD detection >0 in bone marrow (BM) was highly associated with relapse. B-cell recovery [signifying loss of functional chimeric antigen receptor (CAR) T cells] within the first year of treatment was associated with a hazard ratio (HR) for relapse of 4.5 [95% confidence interval (CI), 2.03–9.97; $P < 0.001$]. Multivariate analysis at day 28 showed independent associations of BMNGS-MRD >0 (HR = 4.87; 95% CI, 2.18–10.8; $P < 0.001$) and B-cell recovery (HR = 3.33; 95% CI, 1.44–7.69; $P = 0.005$) with relapse. By 3 months, the BMNGS-MRD HR increased to 12 (95% CI, 2.87–50; $P < 0.001$), whereas B-cell recovery was not independently predictive (HR = 1.27; 95% CI, 0.33–4.79; $P = 0.7$). Relapses occurring with persistence of B-cell aplasia were largely CD19$^-$ (23/25: 88%). Detectable BMNGS-MRD reliably predicts risk with sufficient time to consider approaches to relapse prevention such as hematopoietic cell transplantation (HCT) or second CAR-T cell infusion.

SIGNIFICANCE: Detectable disease by BMNGS-MRD with or without B-cell aplasia is highly predictive of relapse after tisagenlecleucel therapy for ALL. Clonotypic rearrangements used to follow NGS-MRD did not change after loss of CD19 or lineage switch. High-risk patients identified by these biomarkers may benefit from HCT or investigational cell therapies.

See related commentary by Ghorashian and Bartram, p. 2.

INTRODUCTION

Treatment with tisagenlecleucel has led to long-term remission in up to 50% of children and young adults with relapsed or refractory acute lymphoblastic leukemia (ALL) who were previously rarely curable (1). This autologous, targeted immunocellular therapy has also led to a paradigm shift in therapeutic choices: Prior to availability of tisagenlecleucel, curative approaches to multiply relapsed/refractory ALL ended in treatment with allogeneic hematopoietic cell transplantation (HCT) in the fraction of patients who were able to achieve good remission and qualify for transplant (2). Following tisagenlecleucel treatment, however, there is a percentage of patients who have long-term remissions without further therapy, the longest of which has exceeded 9 years (3).

Second-generation chimeric antigen receptor (CAR) T cell therapies using 4-1BB costimulation have led to minimal residual disease (MRD)–negative remissions by multiparameter flow cytometry (MFC) in approximately 80% to 97% of patients treated (1, 4–6). Although high percentages achieve remission, a portion of patients will lose their CAR T cells within a few months. B-cell aplasia is a marker of functional CD19 CAR persistence, so B-cell recovery/loss of B-cell aplasia suggests loss of functional CAR-T cells. Other patients will relapse in spite of CAR-T persistence as a result of CD19 escape, either from mutated CD19 splice variants that are no longer recognized by tisagenlecleucel, genetic mutations in CD19 that lead to truncated proteins with loss of surface antigen, or lineage switch in blasts with loss of CD19 (7, 8). With these issues in mind, a challenge in managing patients

[1]Section of Transplantation and Cellular Therapy, Children's Hospital Los Angeles Cancer and Blood Disease Institute, USC Keck School of Medicine, Los Angeles, California. [2]Novartis Pharmaceuticals Corporation, East Hanover, New Jersey. [3]Department of Pediatrics, Perelman School of Medicine, University of Pennsylvania, Philadelphia, Pennsylvania. [4]Division of Oncology, Center for Childhood Cancer Research and Cancer Immunotherapy Program, Children's Hospital of Philadelphia, Philadelphia, Pennsylvania. [5]Department of Pediatrics, The University of Texas Southwestern Medical Center, Dallas, Texas. [6]Department of Pediatrics, Emory University School of Medicine, Atlanta, Georgia. [7]Aflac Cancer and Blood Disorders Center, Healthcare of Atlanta, Atlanta, Georgia. [8]Pediatric Hematology, Hospital Sant Joan de Déu de Barcelona, Fundació Sant Joan de Déu, Barcelona, Spain. [9]Department of Pediatrics and Internal Medicine, University of Utah, Salt Lake City, Utah. [10]Department of Pediatrics, Graduate School of Medicine, Kyoto University, Kyoto City, Japan. [11]Michigan Medicine Bone Marrow Transplant and Leukemia, C.S. Mott Children's Hospital, Ann Arbor, Michigan. [12]Pediatric Blood and Marrow Transplant, Duke University Medical Center, Durham, North Carolina. [13]Pediatric Hematology and Oncology, Children's Mercy Hospital; University of Missouri—Kansas City School of Medicine, Kansas City, Missouri. [14]Division for Stem Cell Transplantation, Immunology and Intensive Care Medicine Hospital for Children and Adolescents University Hospital Frankfurt, Frankfurt, Germany. [15]Pediatric Hemato-Immunology Department, Hôpital Universitaire Robert Debré (APHP), Paris, France. [16]Université de Paris et Institut de Recherche Saint-Louis (EA3518), Paris, France. [17]Department of Pediatric Hematology and Oncology, Oslo University Hospital, Oslo, Norway. [18]Department of Pediatrics, The University of Minnesota Medical School, Minneapolis, Minnesota. [19]Novartis Pharmaceuticals Corporation, Basel, Switzerland.

Note: Supplementary data for this article are available at Blood Cancer Discovery Online (https://bloodcancerdiscov.aacrjournals.org/).

M.A. Pulsipher and X. Han are co-first authors of this article.

Current address for M.A. Pulsipher: Pediatric Hematology and Oncology, Children's and Adolescent Cancer Initiative at Huntsman Cancer Institute and Intermountain Primary Children's Hospital, Huntsman Cancer Institute at the University of Utah, Salt Lake City, Utah.

Corresponding Author: Michael A. Pulsipher, Huntsman Cancer Institute at the University of Utah, 2000 Circle of Hope Drive, Salt Lake City, UT 84112. Phone: 323-361-8840; Fax: 323-361-8068; E-mail: michael.pulsipher@hci.utah.edu

Blood Cancer Discov 2022;3:66–81

doi: 10.1158/2643-3230.BCD-21-0095

This open access article is distributed under Creative Commons Attribution-NonCommercial-NoDerivatives License 4.0 International (CC BY-NC-ND).

©2021 The Authors; Published by the American Association for Cancer Research

with ALL CAR-T is that there are not reliable markers to predict relapse. This has led some to propose allogeneic HCT for all patients early after CAR-T cell therapy to minimize relapse risk (9, 10)

MRD is currently used for risk stratification of patients with ALL receiving chemotherapy and HCT (11, 12). The Children's Oncology Group has a standardized MFC assay that detects disease reliably in marrow or peripheral blood at levels ≥0.01% of mononuclear cells (11). More sensitive MRD assays use detection of specific immunoglobulin (Ig)H or T-cell receptor rearrangements, either by allele-specific polymerase chain reaction (PCR) or by next-generation sequencing (NGS). The NGS-MRD approach has been shown to reliably detect blasts at levels ≤10^{-6} cells (13). Using this approach, children with ALL at very low risk of relapse after chemotherapy or HCT can be identified (14, 15). Published data of NGS-MRD in CAR-T cell therapy for ALL are limited to a single study: The Fred Hutchinson group showed improved event-free survival (EFS) with NGS negativity at a single time point (D21) after infusion of CAR-T cells in 28 adult patients (16). The prognostic value of NGS-MRD has not been demonstrated in pediatric and young adult patients treated with tisagenlecleucel, or with assessments over time.

On the basis of our hypothesis that MRD measurements at various time points after achieving remission with tisagenlecleucel could identify patients at high or low risk of relapse after CAR-T cell therapy, we analyzed blood and marrow samples from patients enrolled in the ELIANA and ENSIGN trials and compared MFC-MRD with NGS-MRD. We also looked at the influence of the presence or absence of B-cell aplasia and its effect on predictive models for patient outcome. Finally, we compared several distinct patterns separating $CD19^-$ relapse from $CD19^+$ relapse.

RESULTS

Population and MRD Sampling

A total of 1,771 MFC samples were analyzed from 143 patients enrolled in the ENSIGN and ELIANA studies (median follow-up 38.4 months). A total of 474 samples from 109 patients were analyzed for NGS-MRD. A total of 426 (90%) passed quality control, including 125 blood and 301 bone marrow (BM) samples. Time points were from screening to 24 months after infusion, with 79% of postinfusion samples drawn at 1, 3, and 6 months (Supplementary Table S1A and S1B). The MFC analysis was a scheduled part of the trials and performed centrally on fresh samples, whereas the NGS-MRD analysis was *post hoc* and performed on frozen samples from the same blood and marrow draws. Ninety-five percent of baseline blast samples allowed identification of a tumor clone by NGS-MRD. A total of 387 samples were informative for both MFC and NGS-MRD.

There are no significant differences between the subgroup of patients with NGS-MRD samples available compared with those without (Table 1) except for a trend toward fewer patients with prior HCT in the non-NGS group. Notably, the patients undergoing this analysis were a very high-risk population, with 58% relapsed after a previous allogeneic HCT and 69% with high marrow tumor burden (blast count and/or flow MRD ≥50%) at enrollment.

Sensitivity of MFC-MRD and NGS-MRD in BM and Blood

To define the relative sensitivity of ALL blast detection in blood and marrow by MFC-MRD and NGS-MRD sampling, we compared the results of the different methods in the same samples. As expected, MFC-MRD detected a higher percentage of blasts in BM compared with peripheral blood (Fig. 1A). This was also true in NGS samples, wherein BMNGS-MRD detection was approximately one log higher (Fig. 1B). BMNGS-MRD resulted in comparable detection to BMMFC-MRD at levels above 10^{-4}, but as expected, NGS-MRD was much more sensitive, showing high numbers of samples that were NGS-MRD positive (MRD^+) but MFC-MRD negative (MRD^-; Fig. 1C). In a further comparison of peripheral blood NGS-MRD with BMMFC-MRD, we noted that peripheral blood NGS-MRD was more sensitive at detecting disease (Fig. 1D): 9% (7/77) more samples were detected by peripheral blood NGS-MRD at a sensitivity level of 10^{-6} than those detected by BMMFC-MRD, with 13% (10/77) more detected if any level of detection was allowed compared with MFC-MRD of marrow. This means that 10 patients had detectable peripheral blood NGS-MRD but negative BMMFC-MRD, which was clinically meaningful as 5 developed BM/extramedullary relapse, 4 received HCT/additional therapy, and 1 was lost to follow-up.

Figure 1E and F give insight into the concordance of MFC-MRD with NGS-MRD and the increased sensitivity of NGS-MRD. MFC-MRD limit of sensitivity is 10^{-4}, whereas NGS-MRD provides reliable sensitivity of ≥10^{-6}. NGS-MRD can be reported with sensitivity cutoffs that vary depending on the level of sensitivity desired and the cell numbers provided. The 151 baseline and postinfusion samples detected as positive by MFC assessment aligned well with NGS-MRD results (Pearson r of 0.81). In addition, for 287 postinfusion samples (from 95 patients) with both NGS and MFC results available, MFC detected 18% (51/287) as MRD^+, whereas NGS detected 22% (62/287), 29% (82/287), 33% (96/287), and 41% (118/287) as MRD^+ at sensitivity cutoff levels of 10^{-4}, 10^{-5}, 10^{-6}, and any detectable level (which may roughly correspond to 10^{-7}), respectively. There were 88% more samples detected by NGS than those detected by MFC (96 vs. 51) if a sensitivity level of 10^{-6} was used, and 131% more detected (118 vs. 51) when including samples with any detectable disease. Notably, there were no samples that were $MFC\text{-}MRD^+$ and $NGS\text{-}MRD^-$.

Data shown in Fig. 1E and F demonstrate that that there are many cases for which disease was detected by NGS-MRD and not by flow, with the corresponding data points visible close to the y-axis. Notably, a detection sensitivity cutoff of 10^{-6} excludes many positive samples below this level. To distinguish sample groups including any level of detectable disease from higher cutoff levels such as 10^{-4} or 10^{-6}, they were designated as NGS-MRD >0, whereas samples negative for any detectable disease were designated as NGS-MRD = 0. One patient had a relapsed sample with 28% MRD in blood by NGS but not detected by BMMFC. This patient experienced a morphologic relapse with no B-cell markers, consistent with lineage switch [had previously had a mixed-lineage leukemia (*MLL*) rearrangement], and the relapse was missed by MFC.

Table 1. Baseline patient characteristics in the NGS and non-NGS cohorts

	NGS population (*n* = 109)	Non-NGS population (*n* = 34)	*P*	Overall population (*N* = 143)
Age, years, *n* (%)				
<10	39 (35.8)	13 (38.2)	0.128	52 (36.4)
≥10 to <18	48 (44.0)	19 (55.9)		67 (46.9)
≥18	22 (20.2)	2 (5.9)		24 (16.8)
Median (min, max)	12 (3, 25)	12 (4, 18)		12 (3, 25)
Sex, *n* (%)				
Female	51 (46.8)	17 (50.0)	0.845	68 (47.6)
Male	58 (53.2)	17 (50.0)		75 (52.4)
Race, *n* (%)				
Asian	11 (10.1)	4 (11.8)	0.943	15 (10.5)
Other	14 (12.8)	4 (11.8)		18 (12.6)
White	84 (77.1)	26 (76.5)		110 (76.9)
Number of previous lines of therapy, median (min, max)	3 (1, 9)	3 (1, 6)		3 (1, 9)
Complex karyotypes (≥5 abnormal), *n* (%)				
No	75 (68.8)	23 (67.6)	1	98 (68.5)
Yes	34 (31.2)	11 (32.4)		45 (31.5)
Down syndrome				
No	101 (92.7)	32 (94.1)	1	133 (93.0)
Yes	8 (7.3)	2 (5.9)		10 (7.0)
Refractory/relapse status at study entry, *n* (%)				
Primary refractory	8 (7.3)	5 (14.7)	0.191	13 (9.1)
Relapsed disease	101 (92.7)	29 (85.3)		130 (90.9)
Prior HCT, *n* (%)				
No	46 (42.2)	21 (61.8)	0.051	67 (46.9)
Yes	63 (57.8)	13 (38.2)		76 (53.1)
Enrollment BM tumor burden, *n* (%)				
High	75 (68.8)	23 (67.6)	1	98 (68.5)
Low	34 (31.2)	11 (32.4)		45 (31.5)
LD chemotherapy group, *n* (%)				
Fludarabine based	103 (94.5)	31 (91.2)	0.393	134 (93.7)
No LD chemotherapy	4 (3.7)	3 (8.8)		7 (4.9)
Non–fludarabine based	2 (1.8)	0 (0)		2 (1.4)

NOTE: *P* values comparing subgroup differences between NGS and non-NGS populations are from Fisher exact test.

Abbreviation: LD, lymphodepleting.

MRD Detection and Time to Relapse in the Context of NGS-MRD Detection Quality and Quantitation

NGS-MRD assays can be reported out at specific cutoff levels to ensure a high level of confidence that a threshold level of disease is present. To reach that level of confidence, a reasonable number of cells and a specific quality of DNA need to be included. As we analyzed our NGS-MRD data, we noted that a number of patients had detectable disease, but because values did not reach thresholds required for the limit of detection (LOD) or limit of quantitation (LOQ), they were not reported out as positive for the 10^{-6} cutoff (Fig. 2A, left). The right panel of Fig. 2A illustrates that the LOD and LOQ can vary several logs. For samples with high blast counts, this is not an issue, and definitive values can be reported, but at these very low disease levels, the percentage of samples with disease detected that fall below LOD or LOQ increases. To investigate the clinical relevance of samples with <LOD/LOQ MRD levels, we analyzed outcomes of 19 responding patients with NGS-MRD$^+$ disease below the 10^{-6} cutoff. Fourteen of them relapsed or became MFC-MRD$^+$, four were censored for additional therapy, and only one had an ongoing remission (Supplementary Fig. S1).

To assess the lead time different MRD approaches give prior to relapse, we compared the time between the first observation of MFC-MRD, NGS-MRD at a sensitivity of 10^{-6}, and NGS-MRD detectable below the 10^{-6} cutoff in patients who eventually relapsed (Fig. 2B). With the sampling schedule associated with this protocol (BM at 1, 3, 6, 9,

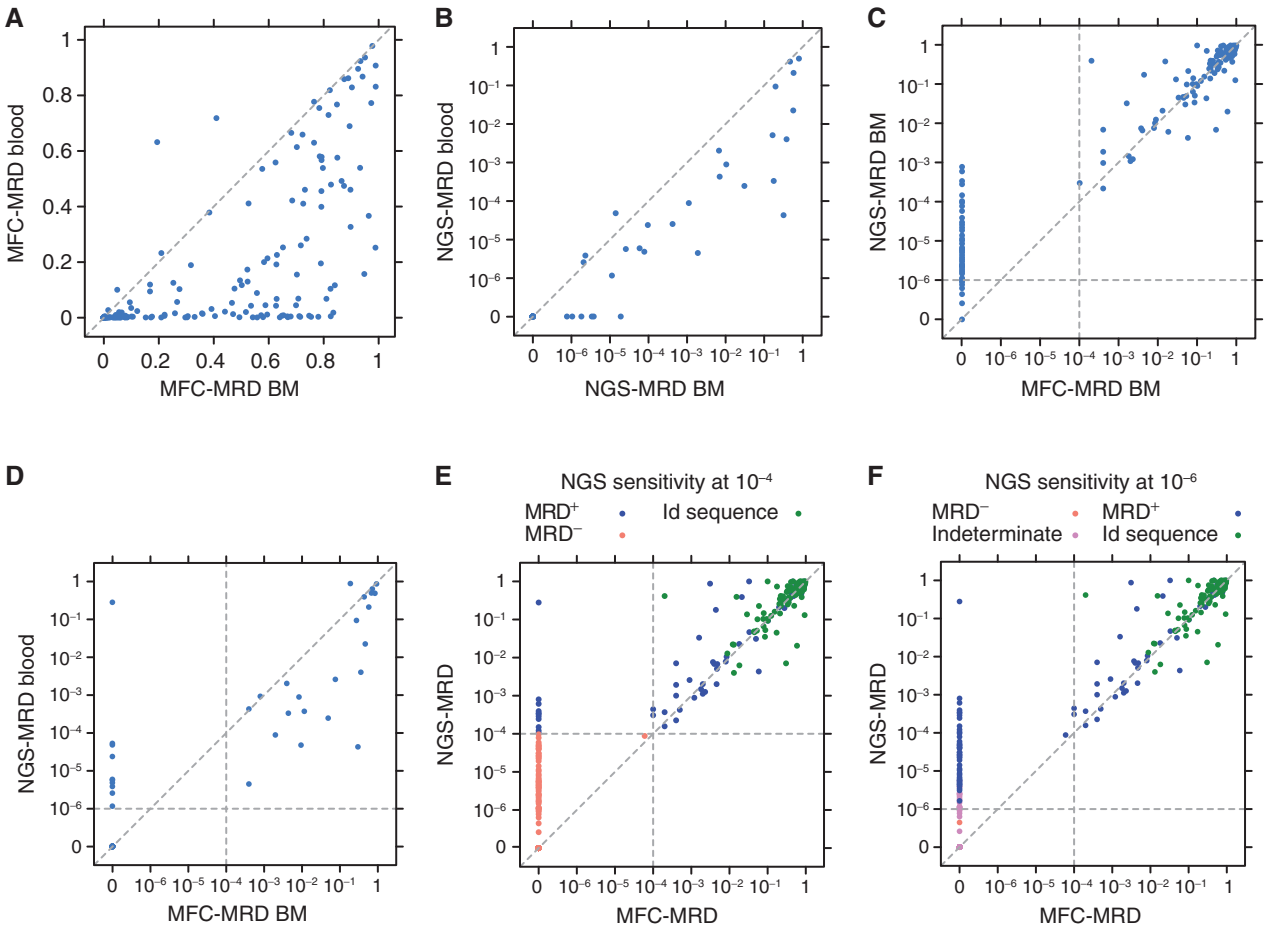


Figure 1. Comparisons of the sensitivity of MFC-MRD and NGS-MRD from peripheral blood and BM. Vertical and horizonal dotted lines represent the sensitivity cutoff for MFC and NGS, respectively. **A,** MFC-MRD from blood (*y*-axis) compared with samples from the same time point obtained from BM (*x*-axis); $n = 450$. **B,** NGS-MRD from blood (*y*-axis) compared with samples from the same time point obtained from BM (*x*-axis); $n = 66$. **C,** NGS-MRD from BM (*y*-axis) compared with MFC-MRD from BM (*x*-axis) in all matched samples; $n = 280$. **D,** NGS-MRD from blood (*y*-axis) compared with MFC-MRD from BM (*x*-axis) in all matched samples; $n = 77$. **E,** NGS-MRD compared with MFC-MRD in all matched samples with an NGS sensitivity cutoff of 10^{-4}. **F,** NGS-MRD compared with MFC-MRD in all matched samples with an NGS sensitivity cutoff of 10^{-6}. **E** and **F**, Green, red, blue, and purple dots represent baseline index clones, NGS-MRD$^-$, NGS-MRD$^+$, and NGS-MRD indeterminate (insufficient number of cells to determine MRD), respectively.

and 12 months), relapse was noted without previous MRD detection in 50% of patients by MFC, 31% of patients by NGS-MRD at a sensitivity of 10^{-6}, and 0% of patients with NGS-MRD detectable below the 10^{-6} level. For those whose MRD was detected prior to overt relapse, the median time to relapse was 52 (range, 14–86) days from first MFC-MRD detection, 70 (range, 15–196) days from NGS-MRD detected above 10^{-6}, and 168 (range, 47–330) days from detection in patients with detectable NGS-MRD below the 10^{-6} cutoff. This shows that the more sensitive NGS measurements detect disease at levels that offer sufficient lead time prior to overt relapse to allow repeat sampling and/or coordination of therapeutic interventions.

Predictive Power of BMMFC-MRD and BMNGS-MRD

Patients who achieved complete remission (CR)/CR with incomplete hematologic recovery (CRi) but did not achieve BMMFC-negative remission at day 28 and/or month 3 after tisagenlecleucel infusion did poorly. Of 109 day 28 CR patients, 2 were BM MRD$^+$ by MFC. These patients relapsed on day 80 and day 85, and died without additional therapy. There were 5 of 82 patients who achieved CR/CRi by 3 months and were BMMFC-MRD$^+$. Two went on to relapse at day 92 and day 106, one underwent HCT (day 93), one received other therapy at day 151, and one was lost to follow-up at day 86.

For patients who were able to achieve CR/CRi, we hypothesized that measures of BMNGS-MRD and B-cell aplasia at key time points after tisagenlecleucel infusion would allow us to more accurately predict risk of relapse and overall survival (OS). We started by analyzing BMNGS-MRD$^+$ patients who were considered positive at a cutoff of 10^{-6} versus all patients with measurements that did not meet this cutoff (BMNGS-MRD >0; Fig. 3A and B). Surprisingly, the EFS and OS for these two groups were not significantly different ($P = 0.53$ and $P = 0.46$, respectively). We noted that there were 10 NGS-MRD$^+$ measurements with a sensitivity cutoff of 10^{-6} in this cohort, but there were another 10 patients with NGS-MRD >0

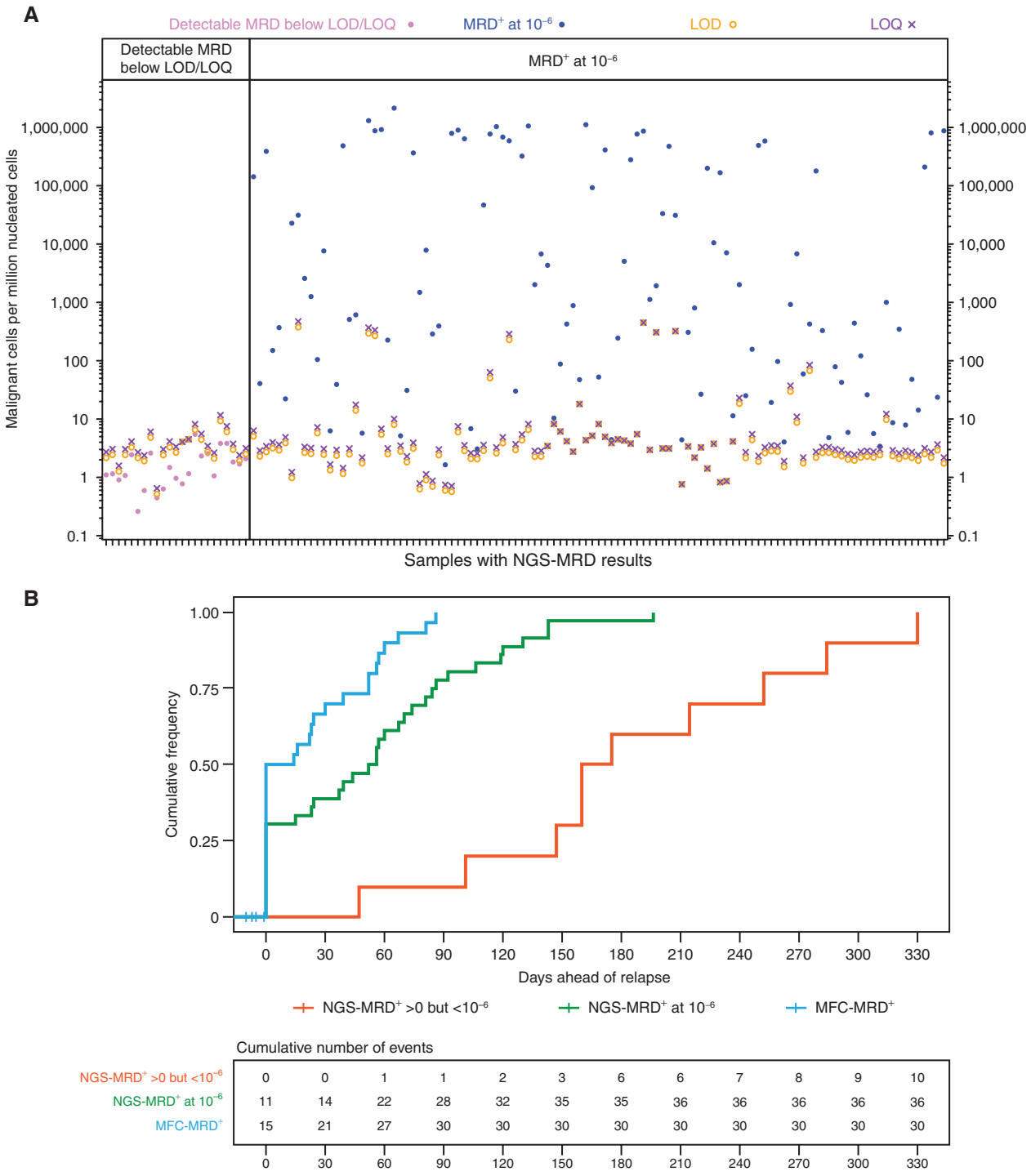


Figure 2. Characteristics of NGS-reported MRD values and their associated lead times ahead of clinical relapse. **A,** Characteristics of reported values for BMNGS-MRD; *x*-axis represents individual samples, and *y*-axis represents a quantitative measure of MRD (normalized number of malignant cells in 1 million nucleated cells). For each sample, there is an LOD (shown by an orange circle) and an LOQ (shown by a purple ×). These quantities are directly proportional to the number of cells provided to the assay; samples with higher numbers of input cells allow more reliable detection and quantitation of residual disease at low levels. Positive test values below the LOD suggest that although residual disease is likely present, it might not be observed again if a repeat test of the same sample source (blood or marrow) were sent. Positive test values below the LOQ imply that the reported MRD frequencies may be inaccurate, although such values may be of the correct order of magnitude. The left panel shows samples that were detectable but below the LOD and LOQ, whereas the right panel shows samples that were considered positive (above LOD and LOQ) at the cutoff level of 10^{-6}. **B,** Cumulative frequencies to overt relapse after patients achieved MFC-MRD$^+$ (blue line), NGS-MRD$^+$ at 10^{-6} level (green), and NGS-MRD$^+$ below the 10^{-6} level but still detectable (red) were plotted using the Kaplan–Meier method.

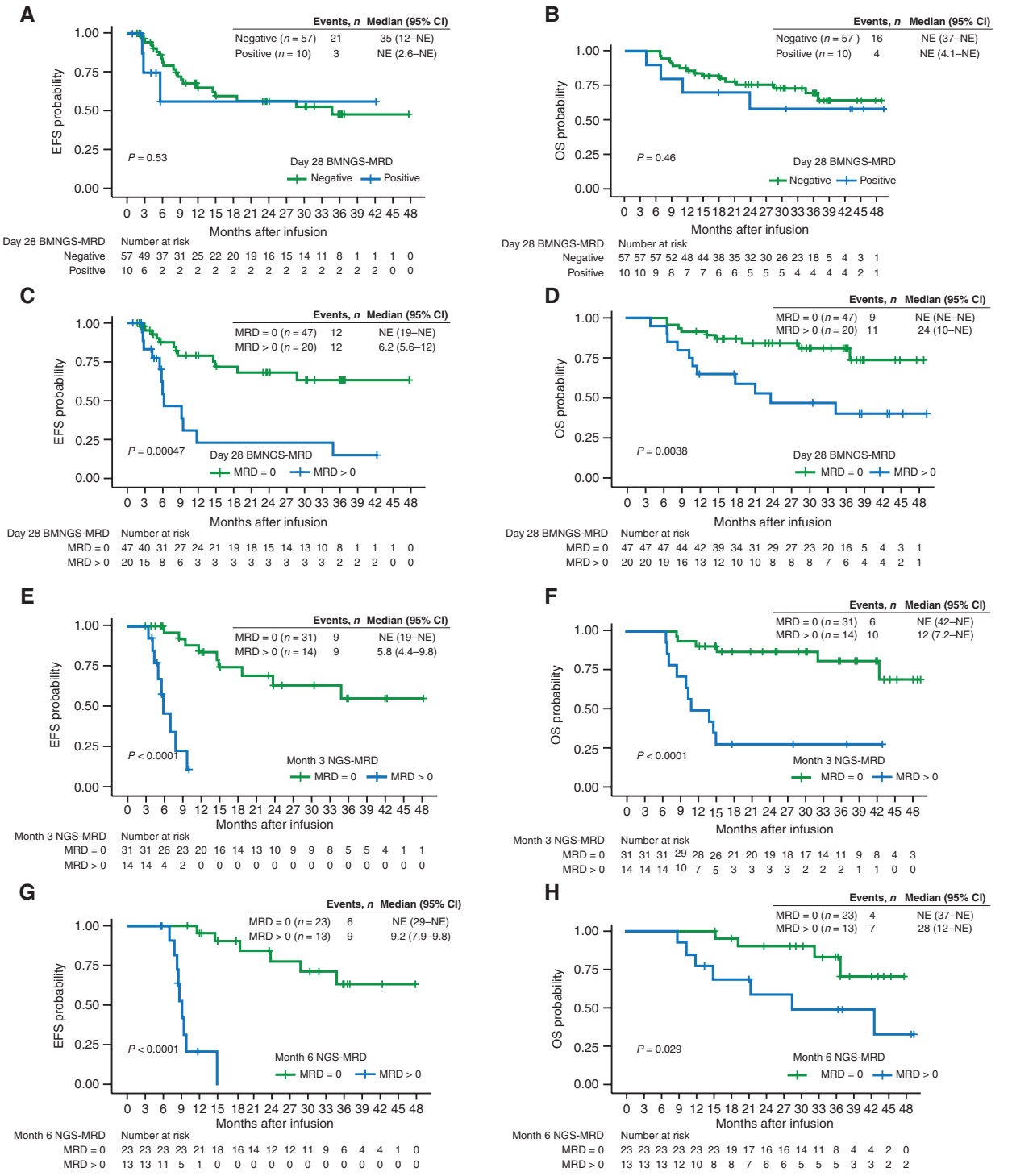


Figure 3. CR/CRi patients with detectable BMNGS-MRD at the end of day 28, month 3, and month 6 after tisagenlecleucel therapy had significantly shorter EFS and OS by Kaplan–Meier analyses, with the log-rank test *P* values included. EFS (**A**) and OS (**B**) of responding patients with BMNGS-MRD$^-$ based on cutoff of 10^{-6} at day 28 (green line) versus those with BMNGS-MRD$^+$ (blue lines). EFS (**C**) and OS (**D**) of responding patients based on detection of BMNGS-MRD at 28 days at any level (blue lines) compared with patients with BMNGS-MRD = 0 (green lines). EFS (**E**) and OS (**F**) of responding patients based on detection of NGS-MRD at 3 months at any level (blue lines) compared with patients with BMNGS-MRD = 0 (green lines). EFS (**G**) and OS (**H**) of responding patients based on detection of BMNGS-MRD at 6 months at any level (blue lines) compared with patients with BMNGS-MRD = 0 (green lines). CI, confidence interval; NE, not estimable.

at day 28 (Fig. 1F). To assess the impact of increased sensitivity of our NGS-MRD testing, we analyzed the dataset with a comparison of NGS-MRD = 0 versus NGS-MRD >0, which included any level of detection (Fig. 3C and D). This led to a dramatic improvement in our ability to determine populations at higher and lower risk of relapse (NGS-MRD = 0 EFS of 68% [95% confidence interval (CI), 54–86] at 2 years versus 23% (95% CI, 8.8–62) for NGS-MRD >0 ($P = 0.00047$). Lower relapse rate led to much higher OS in this cohort [2-year OS with NGS-MRD = 0 of 84% (95% CI, 74–96) vs. 47% (95% CI, 29–77) for NGS MRD >0; $P = 0.0038$].

The lower curve of Fig. 3C suggests that a small percentage of patients with BMNGS-MRD$^+$ disease at day 28 may have longer term remissions. To analyze this in more detail, we looked at patients who were BMNGS-MRD >0 who either stayed positive or who became negative at later time points. The prognosis of patients with consecutive BMNGS-MRD >0 tests was uniformly poor. Of 26 patients with consecutive BMNGS-MRD >0 tests, 19 relapsed, 6 were censored for HCT or other new cancer therapies because of B-cell recovery and/or BMMFC-MRD$^+$, and 1 was lost to follow-up. Prognosis of those with a BMNGS-MRD >0 test followed by subsequent BMNGS-MRD = 0 results was mixed. Of four patients with BMNGS-MRD >0 at day 28 who turned MRD = 0 at month 3 and remained 0 at later time points, two had ongoing CR (>40 months), one had a late CD19$^-$ relapse at day 1,057, and one had HCT at day 140 for the indication of early B-cell recovery. CAR transgene levels in the blood in these four patients were well above detectable levels (>1,500 copies/μg gDNA) at day 28. Of three patients with BMNGS-MRD >0 at day 28, NGS-MRD = 0 at month 3, and BMNGS-MRD >0 at month 6, two relapsed and one was censored for HCT. These three patients had low or minimal blood CAR transgene levels by month 6 (two undetectable, and one with 40 copies/μg gDNA). In summary, although patients with two BMNGS MRD >0 values had extremely poor outcomes, a positive test followed by sequential negative tests could sometimes identify long-term survivors without further therapy.

At 3 and 6 months after infusion, a similar predictive power for less relapse and better OS could be shown for patients with BMNGS-MRD = 0 (Fig. 3E–H). Notably, at 3 and 6 months, those with any detectable NGS-MRD disease had a dismal outcome. Of 14 with NGS-MRD >0 at month 3, 9 relapsed between month 4 and month 10 (all dying by month 15), 3 went to HCT (all alive) and 2 received additional cancer therapy (1 relapsed shortly thereafter and died, and 1 remained alive at last follow-up). Of 13 with NGS-MRD >0 at month 6, 9 relapsed between month 7 and month 15, 1 went to HCT and remains alive at last follow-up, and 3 went on to have additional cancer therapy (2 alive and 1 lost to follow-up). No one with NGS-MRD >0 detected at these later time points survived without significant additional intervention. At 3 and 6 months, using positive BMNGS-MRD with a cutoff of 10^{-6} was predictive of poor outcome (Supplementary Fig. S2A–S2D), but the best predictor at all time points was using a cutoff of NGS-MRD >0.

To determine the specificity of very low levels of NGS-MRD, we analyzed the MRD-defining sequences of 22 samples from 19 patients with MRD detected below LOD/LOQ 10^{-6} cutoffs compared with the Adaptive "uniqueness" database. All 21 of the unique sequences from this cohort (17 *IgH VDJ*, 1 *IgH DJ*, 2 *IgK*, and 1 *IgL*) fell into the "most unique" category, with probability scores ranging from 7.5×10^{-8} to 2.4×10^{-41}. To calculate the specific risk of false positives in our cohort, we assessed whether the MRD-defining sequences of these 19 patients were detected at any level in the 316 MRD samples run for this study. The false-positive rate was calculated as the total number of matches in the nonmatched patients' repertoires divided by the total number of comparisons against nonmatched patients' repertoires [23/6,863; 3.4×10^{-3} (95% CI, 2.2×10^{-3} to 4.9×10^{-3})]. While a rate of less than 1% is reassuring, being less than 1%, because multiple sequences are tracked for each patient, the probability of a false positive with these sequences is much lower.

Predictive Power of the Loss of B-cell Aplasia

We performed Kaplan–Meier analyses of EFS in patients with continued B-cell aplasia versus those who recovered B cells between 1 to 3 months, 3 to 6 months, 6 to 9 months, and 9 to 12 months after tisagenlecleucel infusion. The analysis showed statistically worse outcomes of patients losing B-cell aplasia prior to month 9 (Supplementary Fig. S3A–S3D). Notably, only three patients lost B-cell aplasia between 6 to 9 months and two patients between 9 to 12 months. To quantitate this effect, we built a Cox model for EFS with B-cell recovery as a time-dependent covariate to assess the risk of relapse after a patient had B-cell recovery. As shown in Fig. 4, patients who had B-cell recovery during the first year had significantly higher risk of relapse compared with those without B-cell recovery [hazard ratio (HR) = 4.5; 95% CI, 2.03–9.97; $P < 0.001$; Fig. 4A], with predicted EFS at 2 years of 9% and 14% for those with B-cell recovery at 3 and 6 months, respectively (Fig. 4B). Notably, there is steady improvement in EFS for patients who arrive at 3 through 12 months with persistent B-cell aplasia [Fig. 4C; 2-year EFS values for persistence of B-cell aplasia at 3, 6, 9, and 12 months are 63% (range, 51%–73%), 72% (range, 59%–82%), 83% (range, 70%–91%), and 88% (range, 73%–95%), respectively]. There were six patients who had B-cell recovery after 1 year (from 12–37 months), five with ongoing response (follow-up 18–48 months) without further therapy, and one lost to follow-up at month 23.

Multivariate and Combined Analysis Models

We created multivariate Cox models looking at time-dependent B-cell aplasia versus BMNGS-MRD = 0 at day 28 and month 3 after infusion as risk factors for relapse. At day 28, CR/CRi patients with BMNGS-MRD >0 had a significantly higher risk for relapse compared with those with BMNGS-MRD = 0 (HR = 4.87; 95% CI, 2.18–10.8; $P < 0.001$; Fig. 5A). B-cell recovery within the first year remained an independent risk factor for relapse (HR = 3.33; 95% CI, 1.44–7.69; $P = 0.005$; Fig. 5A and B). Notably, patients with BMNGS-MRD >0 at 3 months had extremely poor outcomes compared with those with BMNGS-MRD = 0 (HR = 12; 95% CI, 2.87–50; $P < 0.001$; Fig. 5C and D). At this point, additional B-cell recovery data did not have an independent impact on subsequent outcomes.

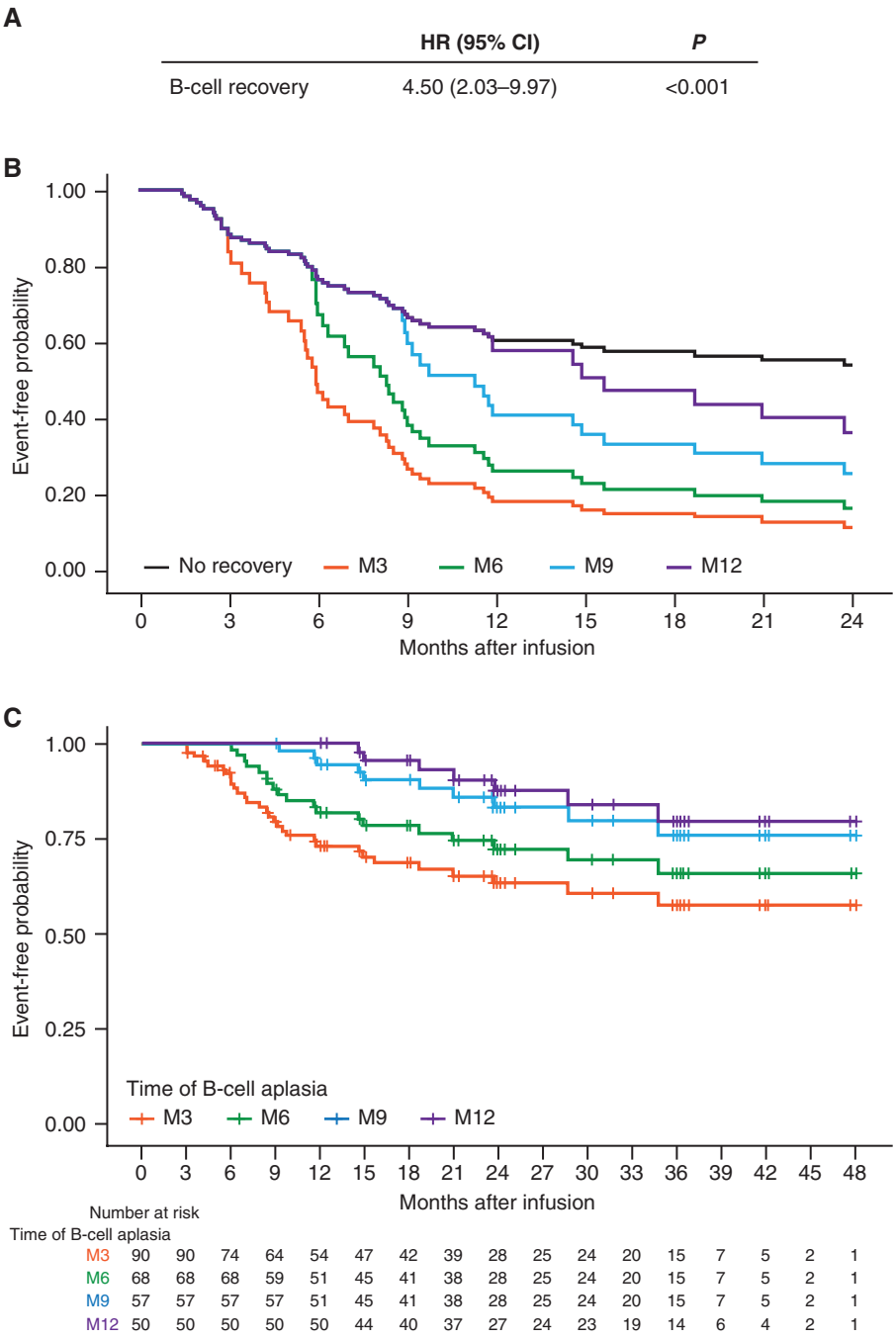


Figure 4. Univariate Cox model to assess the time-dependent effect of B-cell recovery on EFS. **A,** HR, confidence interval, and *P* value for the risk of relapse once patients had B-cell recovery within 1 year after infusion. **B,** Adjusted EFS curves based on the Cox model from **A** for patients with B-cell recovery by month 3 (M3), month 6 (M6), month 9 (M9), and month 12 (M12). **C,** Landmark EFS analysis for patients with persistent B-cell aplasia and reaching M3, M6, M9, and M12.

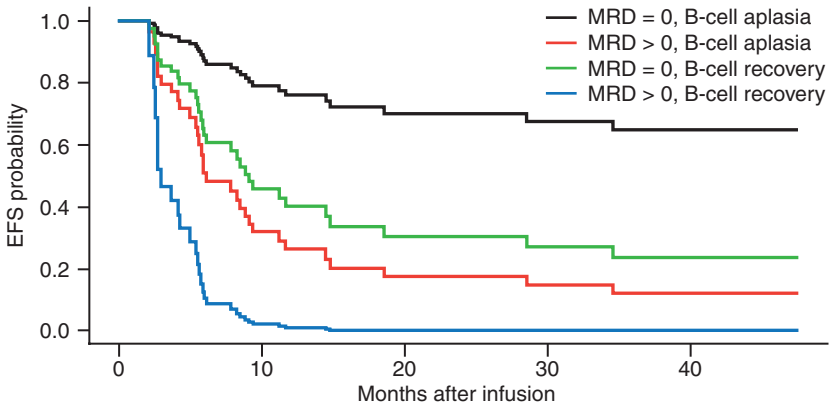
Clinical Associations with CD19$^+$ or CD19$^-$ Relapse

We sought to define possible clinical associations with CD19$^+$ and CD19$^-$ relapse. The timing of CD19$^+$ versus CD19$^-$ relapse largely overlaps, occurring both early and late, with the large majority of relapses occurring within the first year after infusion (Fig. 6A). Notably, B-cell recovery did not have an impact on the timing of CD19$^+$ and CD19$^-$ relapse (Fig. 6B), with a possible exception of a delay in CD19$^+$ relapses in a few patients with persistence of B-cell aplasia (purple line in Fig. 6B). An important result of this analysis, however, is that we show that CD19$^-$ relapse occurs in the setting of persistent B-cell aplasia (Fig. 6C). Twenty-two of the 25 CD19$^-$ relapses occurred in the presence of B-cell aplasia, whereas 11 of the 14 CD19$^+$ relapses occurred after loss of B-cell aplasia. Notably, two of the three

A

	HR (95% CI)	*P*
Day 28 NGS-MRD status		
MRD = 0	—	—
MRD > 0	4.87 (2.18–10.8)	<0.001
B-cell recovery	3.33 (1.44–7.69)	0.005

B



C

	HR (95% CI)	*P*
Month 3 NGS-MRD status		
MRD = 0	—	—
MRD > 0	12.0 (2.87–50.0)	<0.001
B-cell recovery	1.27 (0.33–4.79)	0.7

D

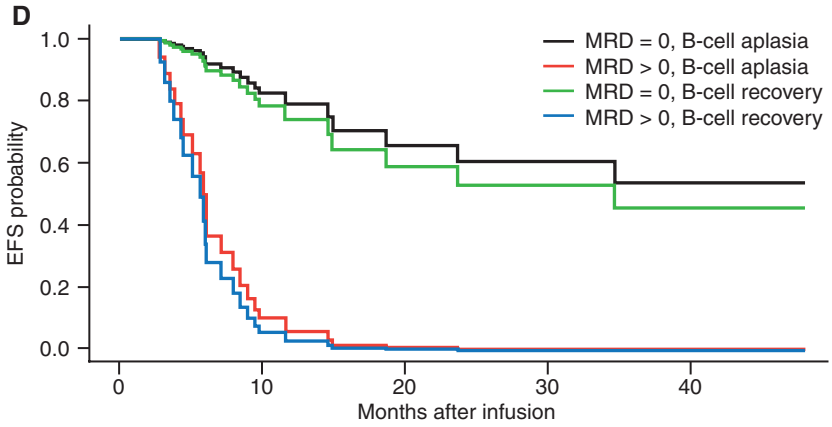
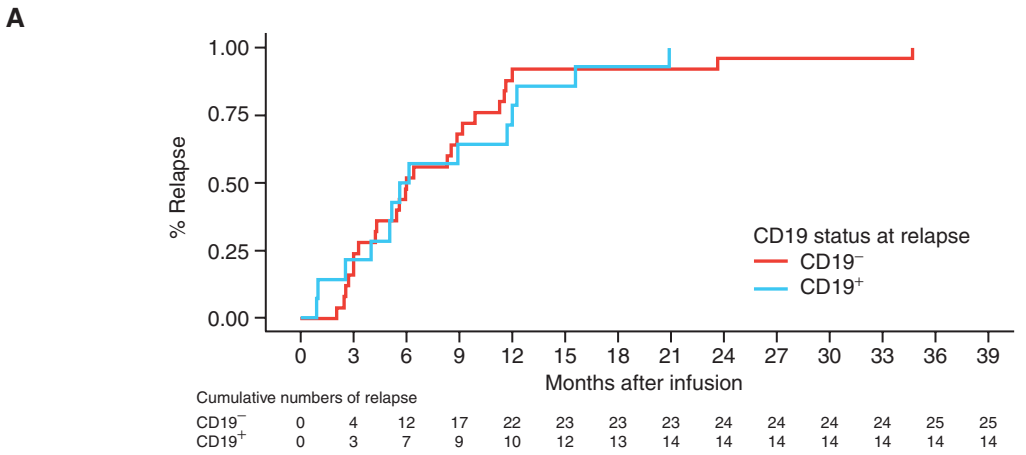
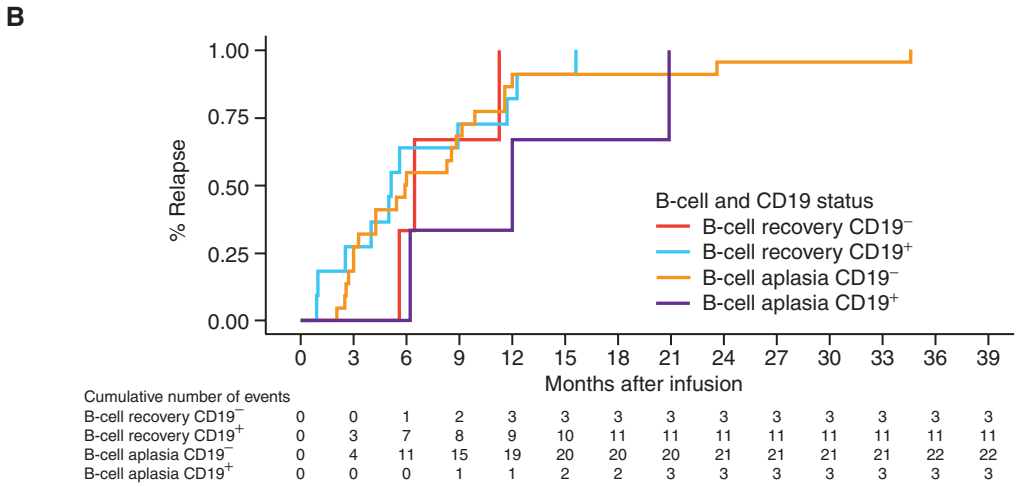


Figure 5. Multivariate Cox proportional hazards analyses for EFS combining BMNGS-MRD status (fixed times at day 28 or month 3) and B-cell recovery (time-dependent covariate). **A,** Results from multivariate Cox model for EFS using day 28 BMNGS-MRD status and B-cell recovery data within the first year ($n = 66$). **B,** Adjusted EFS curves based on the Cox model in **A**. **C,** Results from multivariate Cox model for EFS using month 3 BMNGS-MRD status and B-cell recovery data within the first year ($n = 45$). **D,** Adjusted EFS curves based on the Cox model in **C**.

$CD19^+$ relapses in the context of B-cell aplasia were isolated extramedullary relapses, and the third relapse was $CD19^{dim}$.

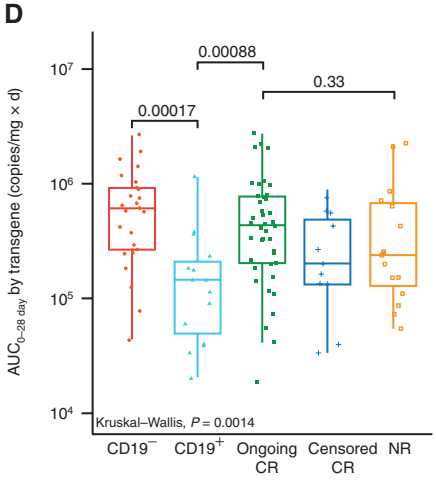
We previously observed that patients experiencing $CD19^+$ relapse had lower CAR-T cell expansion and earlier loss of persistence in contrast to patients with $CD19^-$ relapse (17). We further hypothesized that differing CAR-T cell kinetic profiles might exist between $CD19^+$ and $CD19^-$ relapses. Figure 6D and E show an analysis of whether the area under the curve ($AUC_{0\text{-}28d}$, CAR-T cell exposure during the first 28 days after infusion) and maximal (peak) of expansion kinetics (C_{max}) as measured by transgene levels had an effect on $CD19^-$ or $CD19^+$ relapse frequency. Notably, patients with $CD19^+$ relapse had significantly lower $AUC_{0\text{-}28d}$ and C_{max} compared with patients with $CD19^-$ relapse. Consistent with this finding, there was significantly more grade 3/4 cytokine release syndrome (CRS) in patients with $CD19^-$ relapse (64%, 16/25) compared with those with $CD19^+$ relapse (22%, 3/14; $P = 0.02$). Higher CAR-T cell expansion in patients leads to





C

CD19 status at relapse	B-cell status	
	B-cell recovery	B-cell aplasia
CD19⁻	3 (12%)	22 (88%)
CD19⁺	11 (78%)	3 (22%)



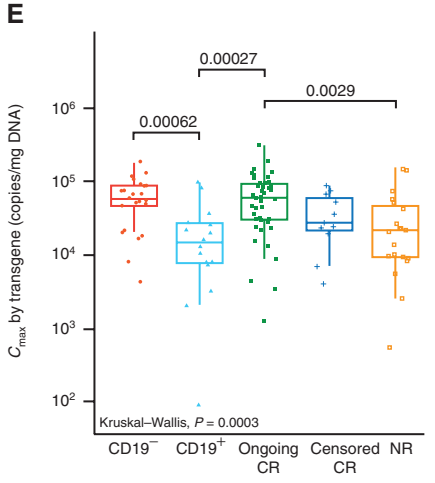


Figure 6. Comparison of time to relapse, B-cell recovery incidence, and tisagenlecleucel expansion in CD19⁻ and CD19⁺ relapse patients. **A,** Kaplan–Meier (KM) analysis for time to relapse by CD19 status: CD19⁻ (red) and CD19⁺ (aqua). **B,** KM analysis for cumulative incidence of relapse by B-cell recovery and CD19 status: B-cell recovery plus CD19⁻ (red), B-cell recovery plus CD19⁺ (green), B-cell aplasia plus CD19⁻ (aqua), and B-cell aplasia plus CD19⁺ (purple). **C,** Relapses according to CD19 status and the presence or absence of B-cell recovery. $AUC_{0\text{–}28d}$ (**D**) and C_{max} (**E**) of transgene levels in patients with CD19⁻ relapse, CD19⁺ relapse, ongoing CR more than 1 year, CR censored for other therapy or HCT within the first year, and nonresponders (NR). Kruskal–Wallis *P* values indicate the significance difference in mean levels among different groups. Numbers above the brackets are pairwise comparison *P* values.

higher grades of CRS (18). In addition. patients with higher disease burden and higher CAR-T cell expansion who have persistent B-cell aplasia are more likely to have CD19$^-$ relapse if relapse occurs. Although tumor burden at enrollment was not different between CD19$^-$ (15 high and 10 low) and CD19$^+$ (11 high and 3 low) relapse patients ($P = 0.31$), these studies did not measure tumor burden at the time of lymphodepleting chemotherapy or just prior to CAR-T cell infusion.

DISCUSSION

In this analysis of combined ELIANA/ENSIGN data, we noted that the large majority (82%) of relapses after tisagenlecleucel occur within the first year after infusion. Given that half of patients treated with tisagenlecleucel have the potential for long-term response/possible cure without HCT, biomarkers defining relapse risk within the first year after infusion could have a major impact, identifying patients for whom HCT or other relapse prevention therapies, including reinfusion, could be considered. We looked at multiple disease, treatment, and demographic characteristics to define appropriate markers and found no effect of age, cytogenic or genetic risk (Supplementary Fig. S4), sex, or prior therapy. While we did observe lower EFS/OS in univariate analysis of patients with high tumor burden at enrollment, the studies did not quantitate tumor burden at time of CAR-T cell infusion, a time point that is likely more clinically meaningful. In addition, tisagenlecleucel was able to induce deep remissions (NGS-MRD = 0) equally well in patients with high or low tumor burdens. Of all the clinical and biological characteristics we analyzed, the most important and actionable risk factors for long-term outcomes were persistence of B-cell aplasia and detection of NGS-MRD.

In practice, B-cell aplasia has been used as a pharmacodynamic indicator of CAR-T functional persistence (5). This was confirmed by our univariate Cox analysis using B-cell recovery as a time-dependent covariate, showing a significant association between B-cell recovery and shorter EFS. However, measuring B-cell aplasia after CAR-T cell treatment by itself is not sufficient to predict relapse, as CD19$^-$ relapse can occur early and at higher frequency in patients with persistence of B-cell aplasia (Fig. 6B and C). Notably, late loss of B-cell aplasia (12 months after CAR-T cell infusion) may have less of a prognostic impact (five of six patients with B-cell recovery after 1 year had ongoing response). Loss of B-cell aplasia varies over time, with the large majority of patients who are going to lose B-cell aplasia doing so prior to 6 months (20 of 31 or 65% of patients with B-cell recovery). After this time point, patients lose B-cell aplasia at a slow rate over subsequent years. Our analysis of loss of B-cell aplasia as a time-dependent variable over the first year after therapy showed a clear decrease in the prognostic importance of the persistence of B-cell aplasia over time. Although we have sufficient numbers to state that loss of B-cell aplasia in the first 6 months leads to poor outcomes, better understanding of the prognostic significance of "late" loss of B-cell aplasia (6–12 months or >1 year after infusion) will require larger patient numbers because it occurs less often.

Measurements of MRD by MFC or PCR are well established in ALL and have been used along with other clinical parameters to guide intensity of therapy (11, 19–21). Presence of pre- and post-HCT MRD guides approaches to HCT and withdrawal of immune suppression (12, 22–24). NGS-MRD testing markedly increases the level of sensitivity in detecting leukemia in the marrow, and this test has been shown to define patients at low risk of relapse when treated with both chemotherapy and HCT (14, 15). In a recent report of pediatric patients with B-cell ALL treated with tisagenlecleucel, the absence of complete MRD response (PCR with ≥10^{-4} sensitivity level), B-cell aplasia, and incidence of CRS was associated with increased cumulative incidence of relapse (25). In this study, we found that MFC-MRD measurements from marrow after CAR-T cell infusion were of limited benefit in spite of having a very high positive predictive value. MFC assessment detected disease quite late; if relapse had not occurred already, there was limited time to plan and initiate therapy to prevent relapse, and outcomes were poor.

Our data show that BMNGS-MRD measurements are the most sensitive biomarker to date for defining risk of relapse after CAR-T cell therapy. It is notable that using LOD and LOQ cutoffs for sensitivity as low as 10^{-6} with the commercially available NGS-MRD assay (Adaptive Biotechnologies), we did not observe the prognostic importance of BMNGS-MRD at day 28 after therapy until we considered any level of detection of NGS-MRD to be high risk. This is likely because CAR-T cells routinely put patients into very deep remissions, but at the same time, any detectable disease at any level using these assays is an indication that the CAR-T cell response may not be sufficient for long-term disease control. At day 28 after infusion, there is a small percentage of patients who have BMNGS-MRD detectable disease who go on to have long-term responses. This may indicate that, in a fraction of patients, the response is not complete at day 28 and may be continuing. Repeat BMNGS-MRD after the initial positive result may help better define risk in patients with low levels of positivity at day 28. Of note, however, by 3 months and at all later time points that we measured up to month 12, any detectable disease by BMNGS-MRD was highly prognostic, and 41 of 42 patients with measurable disease at these later time points in our study either relapsed or were censored for HCT or other therapies.

When measuring NGS-MRD, it is important to understand definitions of LOD/LOQ and the limitations of the assay. The LOD is defined as the malignant cell count at which the assay would detect MRD in 95% of samples. The LOQ is defined as the lowest sample MRD frequency that could be quantitatively determined within 70% relative total error (26). In general, detection of unique clones clearly associated with the patient's blasts is highly specific. When patients have disease detectable under the LOD and LOQ cutoffs, there is a chance that a second BM test from the same patient may not have detected the disease. Because LOD and LOQ are proportional to the number of cells assayed, a simple way to improve our ability to detect disease in this setting would be to be generous with the number of cells sent from BM aspirates (if possible, preferably >10^7 total cells). These limitations also reinforce the value of repeat testing, and underline that optimal frequency and timing of testing after CAR-T cell therapy are not known.

In this study, we also showed that a combination of assessing B-cell aplasia along with BMNGS-MRD measures is important. Patients who lose B-cell aplasia early do poorly. The strongest effect on risk of relapse occurs with B-cell recovery within the first 6 months, and the effect decreases by 12 months (Fig. 4B). Although day 28 measures of NGS-MRD = 0 and B-cell aplasia are independently predictive of good outcomes, by 3 months, NGS-MRD >0 is a powerful predictor of relapse. Although positive BMNGS-MRD predicted relapse in our patients very accurately, negative BMNGS-MRD at a single time point is not sufficient to ensure patients will not relapse, and they should continue to be monitored at intervals over time.

With these data in hand, who should undergo HCT after tisagenlecleucel? It is clear that any patient who loses B-cell aplasia prior to 6 months and who does not have an alternative approach (humanized CAR-T cells, experimental CAR-T cell reinfusions, etc.) has a high probability of relapse. HCT prior to relapse is very reasonable for those eligible for HCT in this population, especially if they have not had a previous HCT. A second group of patients for consideration of HCT or experimental approaches would be those with detectable BMNGS-MRD disease. Those with BMNGS-MRD >0 at 1 month may benefit from a confirmation 2 to 4 weeks later, but those with later measures of BMNGS-MRD >0 may not require confirmation. A population that may or may not benefit from HCT after CAR-T cells is patients who have not had HCT and who fall into a "low-risk" category (they have B-cell aplasia and are BMNGS-MRD = 0). Figure 3C shows that low-risk patients still can relapse [EFS 68% (range, 54%–86%) at 2 years and 64% (range, 48%–83%) at 3 years)]. First HCT in patients with BMNGS-MRD–negative status who are eligible for HCT results in EFS >80% (14). At the same time, sending all such patients to HCT will include patients already destined to do well, for whom the risks of HCT may be unwarranted. Whether these lower risk patients would benefit from HCT requires further study, likely a randomized comparison.

A final intriguing outcome is our observation that continued B-cell aplasia is highly associated with CD19$^-$ relapse. Although this aligns with the mechanism of tisagenlecleucel, the additional observations we make (higher AUC_{0-28d}/C_{max} and grade 3/4 CRS are also highly associated with CD19$^-$ relapse) provide supporting evidence that selective pressure of CAR-T cells, especially where there is higher disease burden, by itself may be important in determining whether patients will have a CD19$^-$ relapse. Some investigators have suggested that CD19$^-$ relapse could be driven by patients coming to CAR-T cell treatment with very low levels of CD19$^-$ mutations present (27). Our cohort included flow assessment that looked for CD19$^-$ clones prior to treatment, and no enrolled patients had clearly defined CD19$^-$ clones; however, this method may not be sufficient to detect very low-level CD19$^-$ clones. Further study of this population, including detailed molecular studies of CD19 mutational status at baseline along with timing and molecular characterization of CD19$^-$ relapses, is underway and will be reported separately. CAR-T cell expansion and high-grade CRS are highly associated with disease burden at time of infusion (6) but may also point to selection pressure from high early CAR-T cell expansion and continuous late exposure as being key to CD19$^-$ relapse. Alternatively, higher disease burden may allow for a higher number of CD19$^-$ clones that may give rise to a CD19$^-$ relapse (6).

This study has important limitations. Although we had nearly 1,800 MFC-MRD measurements, we had just under 500 NGS-MRD assessments. A high percentage of patients had marrow checked at 1 and 3 months, but more limited numbers of patients had samples at 2, 4, or 6 months—times that may also inform clinical decision-making. We also do not have a sufficient number of peripheral blood NGS-MRD samples to adequately define a role for assessing relapse risk by this much more accessible approach. In short, larger numbers, assessment of more time points after CAR-T cell infusion, and comparison of peripheral blood NGS-MRD measurements with BMNGS-MRD measurements will be needed to further refine the use of NGS-MRD as a biomarker to predict relapse. Notably, clonality analyses comparing MRD clones with their corresponding baseline ID clones showed all patients kept the same identifying IgH rearrangements as baseline, with no loss of identifying clonal sequences, regardless of CD19 status. Two patients with *MLL* rearrangement who relapsed with lineage switch also retained their identifying clonal IgH gene rearrangements, confirming that the lineage-switched clones emerged from the previous leukemia.

In conclusion, this study demonstrates that the best biomarker described to date for determining risk of relapse at any given time throughout the first year after CAR-T cell therapy with tisagenlecleucel is NGS-MRD assessment of the marrow with a cutoff of >0 cells detected. B-cell aplasia during the first year is also a strong biomarker, defining patients with possible long-term response. Those who lose B-cell aplasia prior to 6 months or develop NGS-MRD measures >0 on marrow examination are at high risk of relapse, and HCT or other cell or immune therapies should be considered. Whether low-risk patients who have undetectable BMNGS-MRD early on who have not undergone HCT could benefit from early HCT after CAR-T cell therapy is not known and requires further study. How peripheral blood monitoring of NGS-MRD could fit into management of CAR-T cell patients also requires further study.

METHODS

Patient Populations

Two phase II, single-arm, multicenter global studies [ELIANA, *N* = 79 (NCT02435849), data cutoff date July 1, 2019; ENSIGN, *N* = 64 (NCT02228096), data cutoff date May 24, 2019] were conducted including 143 pediatric and young adult patients with CD19$^+$ relapsed or refractory B-cell ALL who were infused with tisagenlecleucel (1). Study protocols were implemented and reported with the ethical principles laid down in the Declaration of Helsinki, and were approved by individual Institutional Review Boards; written informed consents were obtained for all patients. To be eligible for participation in the studies, patients had to be 3 years of age at screening and no older than 21 years of age at diagnosis and have >5% lymphoblasts detected by morphology in BM at screening. Patients who had previously received anti-CD19 therapy were excluded. Eligibility criteria of the two protocols were overlapping with minimal differences (Supplementary

Table S2). CAR-T cells for the first 29 patients in the ENSIGN trial were manufactured by the University of Pennsylvania GMP facility, and the CAR-T cells for the remaining 35 on ENSIGN and all 79 ELIANA patients were manufactured at Novartis. Lymphodepleting chemotherapy was used in 136 of 143 patients before a single infusion of 0.2 to 5×10^6/kg (patients ≤50 kg) or 0.1 to 2.5×10^8 (patients >50 kg) tisagenlecleucel.

MRD Detection by Flow Cytometry

MFC-MRD was measured on fresh blood and BM samples by a central laboratory using a three-tube, eight-color flow cytometry assay with a lower limit of sensitivity of 0.01% of viable white blood cells (WBC). Samples were collected at screening, month 1, month 3, month 6, month 9, and month 12 after infusion. In addition, blood samples were collected weekly during the first month, and at month 1, month 3, month 6, month 9, and month 12. After red blood cell lysis, cells were washed and centrifuged to create a WBC pellet, which was resuspended in wash buffer (PBS + 2% FBS) and aliquoted into flow tubes. Human Fc Receptor Binding Inhibitor (Thermo Fisher Scientific) was added to each tube to reduce nonspecific binding. The suspension was stained with a preprepared qualified antibody cocktail including CD9 (clone M-L13, BD), CD10 (clone HI10a, BD), CD13 (clone WM15, BD), CD19 (clone SJ25C1, BD), CD20 (clone 2H7, BioLegend), CD22 (clone S-HCL-1, BD), CD33 (clone P67.6, BD), CD34 (clone 8G12, BD), CD38 (clone HB7, BD), CD45 (clone HI30, BD), CD58 (clone IC3, BD), CD66c (clone B6.2/CD66, BD), and CD123 (clone 9F5, BD). After incubation, samples were washed, fixed in 0.5% formalin buffer, and acquired on a FACSCanto II cytometer (BD). Data analyses were performed using FCS Express software (De Novo Software).

BM and blood MRD positivity was defined as ≥0.01% leukemic cells out of total viable WBCs. B-cell recovery was defined as the time from onset of remission to the earliest time when blood $CD19^+$ total B cells ≥1% among viable WBCs or ≥3% among lymphocytes.

Ig NGS-MRD Assay

NGS-MRD was measured using ClonoSEQ B-cell Clonality (Adaptive Biotechnologies), an NGS-based assay designed for tumor-specific Ig sequence rearrangement detection. It identifies and tracks rearranged *IgH* (*VDJ*), *IgH* (*DJ*), *IgK*, and *IgL* receptor gene sequences, as well as translocated *BCL1*/*IgH* (*J*) and *BCL2*/*IgH* (*J*) sequences. A subset of BM and blood samples were collected at screening, end of month 1, every 3 months during the first year, and every 6 months during the second year after infusion. Of 117 baseline samples that passed quality control, 111 (95%) had index clones identified. For patients with baseline ID sequences identified, MRD results were reported in postinfusion samples both quantitatively (number of malignant cells per million nucleated cells) and qualitatively (positive or negative at the sensitivity thresholds of 10^{-4}, 10^{-5}, and 10^{-6}, or indeterminate for MRD^- samples with insufficient numbers of assayed cells). In addition, detectable MRD (MRD >0) was defined as any level of MRD regardless of LOD cutoffs to capture those with disease burden below 10^{-6} but higher than 0.

Detection of Tisagenlecleucel Transgene

Detection of tisagenlecleucel transgene DNA and calculation of cellular kinetic parameters [$AUC_{0\text{–}28d}$: expansion and persistence of tisagenlecleucel during the first 28 days; C_{max}: the maximum (peak) expansion of tisagenlecleucel] from peripheral blood samples were described previously (15).

Definition of Relapse

Morphologic relapse was defined as blasts in the blood (≥1%), blasts in BM (≥5%), or any extramedullary disease after CR or CRi. Patients who became MRD^+ (≥0.01% leukemic cells) after remission were defined as MFC-MRD^+ CD19 status at relapse was derived from flow MRD result when a patient first turned MRD^+. Time to relapse is defined as the earlier time of morphologic relapse and/or MFC-MRD^+ when correlated with CD19 status.

Statistical Analysis

All statistical analyses were performed using RStudio (RStudio Team 2019. RStudio: Integrated Development for R. RStudio, Inc.; http://www.rstudio.com/). EFS was the time from tisagenlecleucel infusion to the earliest of death, relapse, or treatment failure. EFS analyses were performed in ongoing responding patients at the end of day 28, month 3, or month 6, with relapse being the only event. EFS was censored at last assessment date for patients without events, lost to follow-up, undergoing new cancer therapy, or undergoing HCT. Kaplan–Meier curves were used to compare EFS and OS in responding patients with known NGS Ig MRD status at landmark times of 1, 3, and 6 months after infusion, and *P* values within BMNGS-MRD subgroups (detectable vs. nondetectable) were calculated using the log-rank test.

A univariate Cox model for EFS analysis was developed using B-cell recovery as a time-dependent covariate to assess the effect of B-cell recovery on relapse starting from the day a patient achieved B-cell recovery. All blood longitudinal B-cell measurements after remission within the first year were included, and categorized as recovery and no recovery based on the criteria mentioned above. Patients who had B-cell recovery at the same day as relapse were treated as no B-cell recovery. Similarly, multivariate Cox models combining day 28 and month 3 BMNGS-MRD status and time-dependent B-cell recovery data were explored. Only patients with EFS longer than 1 month or 3 months were included in these multivariate Cox models.

Authors' Disclosures

M.A. Pulsipher reports personal fees from Novartis during the conduct of the study, as well as personal fees from Novartis, Jasper Therapeutics, Medexus, Equillium, Bellicum, and Mesoblast, and grants, personal fees, and nonfinancial support from Miltenyi and Adaptive outside the submitted work. X. Han reports nonfinancial support from Healthcare Consultancy Group during the conduct of the study, as well as personal fees from Novartis outside the submitted work. S.L. Maude reports grants and personal fees from Novartis Pharmaceuticals during the conduct of the study, as well as personal fees from Wugen and Kite Pharma outside the submitted work. T.W. Laetsch reports grants, personal fees, and nonfinancial support from Novartis during the conduct of the study, as well as grants from Pfizer, grants and personal fees from Bayer, and personal fees from YmAbs Therapeutics, Cellectis, Deciphera, and Jumo Health outside the submitted work. M. Qayed reports personal fees from Novartis outside the submitted work. S. Rives reports personal fees from Novarits, Kite, Cellectis, and Celgene/Bristol Myers Squibb during the conduct of the study, as well as personal fees from Jazz Pharma and Amgen outside the submitted work. G.D. Myers reports other support from Novartis Pharmaceuticals outside the submitted work. P. Bader reports grants and personal fees from Novartis, personal fees from Amgen, and grants from Bristol Myers Squibb during the conduct of the study; grants from Medac, Neovii, and Riemser outside the submitted work; and a patent for MSC-FFM licensed and with royalties paid from Medac. A. Baruchel reports personal fees and nonfinancial support from Novartis during the conduct of the study, as well as grants and personal fees from Servier, and personal fees from Jazz, Celgene, and Amgen outside the submitted work. J. Buechner reports personal fees, nonfinancial support, and other support from Novartis during the conduct of the study. H.E. Stefanski reports other support from Novartis outside the submitted work. K. Nguyen reports employment with Novartis. E.R. Waldron reports employment with Novartis. K. Thudium Mueller

reports other support from Novartis outside the submitted work and was employed with Novartis at the time the work was completed. H.J. Maier reports other support from Novartis outside the submitted work, as well as employment with Novartis Pharma AG, Switzerland. G. Kari reports employment with Novartis. S.A. Grupp reports grants, personal fees, and nonfinancial support from Novartis during the conduct of the study. No disclosures were reported by the other authors.

Authors' Contributions

M.A. Pulsipher: Enrolling and treating patients, gathering data, performing data analysis, interpreting results, writing–original draft, writing–review and editing. **X. Han:** Performing data analysis, interpreting results, writing–review and editing. **S.L. Maude:** Enrolling and treating patients, gathering data, writing–review and editing. **T.W. Laetsch:** Enrolling and treating patients, gathering data, writing–review and editing. **M. Qayed:** Writing–review and editing. **S. Rives:** Enrolling and treating patients, gathering data, writing–review and editing. **M.W. Boyer:** Enrolling and treating patients, gathering data, writing–review and editing. **H. Hiramatsu:** Enrolling and treating patients, gathering data, writing–review and editing. **G.A. Yanik:** Enrolling and treating patients, gathering data, writing–review and editing. **T. Driscoll:** Enrolling and treating patients, gathering data, writing–review and editing. **G.D. Myers:** Enrolling and treating patients, gathering data, writing–review and editing. **P. Bader:** Enrolling and treating patients, gathering data, writing–review and editing. **A. Baruchel:** Enrolling and treating patients, gathering data, writing–review and editing. **J. Buechner:** Enrolling and treating patients, gathering data, writing–review and editing. **H.E. Stefanski:** Enrolling and treating patients, gathering data, writing–review and editing. **C. Kalfoglou:** Writing–review and editing. **K. Nguyen:** Performing data analysis, interpreting results, writing–review and editing. **E.R. Waldron:** Performing data analysis, interpreting results, writing–review and editing. **K. Thudium Mueller:** Writing–review and editing. **H.J. Maier:** Writing–review and editing. **G. Kari:** Writing–review and editing. **S.A. Grupp:** Enrolling and treating patients, gathering data, writing–review and editing.

Acknowledgments

The studies presented herein were sponsored by Novartis Pharmaceuticals Corporation.

The authors sincerely thank the patients enrolled in the ELIANA and ENSIGN studies and their families, as well as the principal investigators, support staff, study site coordinators, data monitoring committee members, and institutional review committee members. The authors also thank Harlan Robins, Paul Fields, and Erik Yusko (all employees of Adaptive Biotechnologies) for their contributions in generating the NGS-MRD data and supporting the interpretation of some aspects of the associated results, as well as David A. James, Lida Pacaud, Andrea Chassot Agostinho, and Chris del Corral. Editorial support was provided by Healthcare Consultancy Group and was funded by Novartis Pharmaceuticals Corporation.

Received June 2, 2021; revised July 29, 2021; accepted November 1, 2021; published first December 1, 2021.

REFERENCES

1. Maude SL, Laetsch TW, Buechner J, Rives S, Boyer M, Bittencourt H, et al. Tisagenlecleucel in children and young adults with B-cell lymphoblastic leukemia. N Engl J Med 2018;378:439–48.
2. Sun W, Malvar J, Sposto R, Verma A, Wilkes JJ, Dennis R, et al. Outcome of children with multiply relapsed B-cell acute lymphoblastic leukemia: a therapeutic advances in childhood leukemia & lymphoma study. Leukemia 2018;32:2316–25.
3. Emily Whitehead Foundation [homepage on the Internet]. Philipsburg (PA): Emily Whitehead Foundation; 2014–2021 [cited 2021 Oct 28]. Available from: https://emilywhiteheadfoundation.org/our-journey/.
4. Gardner RA, Finney O, Annesley C, Brakke H, Summers C, Leger K, et al. Intent-to-treat leukemia remission by CD19 CAR T cells of defined formulation and dose in children and young adults. Blood 2017;129:3322–31.
5. Maude SL, Frey N, Shaw PA, Aplenc R, Barrett DM, Bunin NJ, et al. Chimeric antigen receptor T cells for sustained remissions in leukemia. N Engl J Med 2014;371:1507–17.
6. Kadauke S, Myers RM, Li Y, Aplenc R, Baniewicz D, Barrett DM, et al. Risk-adapted preemptive tocilizumab to prevent severe cytokine release syndrome after CTL019 for pediatric B-cell acute lymphoblastic leukemia: a prospective clinical trial. J Clin Oncol 2021;39:920–30.
7. Sotillo E, Barrett DM, Black KL, Bagashev A, Oldridge D, Wu G, et al. Convergence of acquired mutations and alternative splicing of CD19 enables resistance to CART-19 immunotherapy. Cancer Discov 2015;5:1282–95.
8. Orlando EJ, Han X, Tribouley C, Wood PA, Leary RJ, Riester M, et al. Genetic mechanisms of target antigen loss in CAR19 therapy of acute lymphoblastic leukemia. Nat Med 2018;24:1504–6.
9. Zhang X, Lu XA, Yang J, Zhang G, Li J, Song L, et al. Efficacy and safety of anti-CD19 CAR T-cell therapy in 110 patients with B-cell acute lymphoblastic leukemia with high-risk features. Blood Adv 2020;4:2325–38.
10. Shah NN, Lee DW, Yates B, Yuan CM, Shalabi H, Martin S, et al. Long-term follow-up of CD19-CAR T-cell therapy in children and young adults with B-ALL. J Clin Oncol 2021;39:1650–9.
11. Borowitz MJ, Wood BL, Devidas M, Loh ML, Raetz EA, Salzer WL, et al. Prognostic significance of minimal residual disease in high risk B-ALL: a report from Children's Oncology Group study AALL0232. Blood 2015;126:964–71.
12. Bader P, Salzmann-Manrique E, Balduzzi A, Dalle JH, Woolfrey AE, Bar M, et al. More precisely defining risk peri-HCT in pediatric ALL: pre- vs post-MRD measures, serial positivity, and risk modeling. Blood Adv 2019;3:3393–405.
13. Faham M, Zheng J, Moorhead M, Carlton VE, Stow P, Coustan-Smith E, et al. Deep-sequencing approach for minimal residual disease detection in acute lymphoblastic leukemia. Blood 2012;120:5173–80.
14. Pulsipher MA, Carlson C, Langholz B, Wall DA, Schultz KR, Bunin N, et al. IgH-V(D)J NGS-MRD measurement pre- and early post-allotransplant defines very low- and very high-risk ALL patients. Blood 2015;125:3501–8.
15. Wood B, Wu D, Crossley B, Dai Y, Williamson D, Gawad C, et al. Measurable residual disease detection by high-throughput sequencing improves risk stratification for pediatric B-ALL. Blood 2018;131:1350–9.
16. Hay KA, Gauthier J, Hirayama AV, Voutsinas JM, Wu Q, Li D, et al. Factors associated with durable EFS in adult B-cell ALL patients achieving MRD-negative CR after CD19 CAR T-cell therapy. Blood 2019;133:1652–63.
17. Mueller KT, Waldron ER, Grupp SA, Levine JE, Laetsch TW, Pulsipher MA, et al. Clinical pharmacology of tisagenlecleucel in B-cell acute lymphoblastic leukemia. Clin Cancer Res 2018;24:6175–84.
18. Mueller KT, Waldron E, Sickert D, Grupp SA, Maude SL, Levine JE, et al. Impact of humoral immunogenicity (anti-mCAR19 antibodies) on CTL019 cellular kinetics, efficacy, and safety. Blood 2017;130 (Supplement 1):1281.
19. Conter V, Bartram CR, Valsecchi MG, Schrauder A, Panzer-Grumayer R, Moricke A, et al. Molecular response to treatment redefines all prognostic factors in children and adolescents with B-cell precursor acute lymphoblastic leukemia: results in 3184 patients of the AIEOP-BFM ALL 2000 study. Blood 2010;115:3206–14.
20. Attarbaschi A, Mann G, Panzer-Grumayer R, Rottgers S, Steiner M, Konig M, et al. Minimal residual disease values discriminate between low and high relapse risk in children with B-cell precursor acute lymphoblastic leukemia and an intrachromosomal amplification of chromosome 21: the Austrian and German acute lymphoblastic leukemia Berlin-Frankfurt-Munster (ALL-BFM) trials. J Clin Oncol 2008;26:3046–50.

21. Schrauder A, von Stackelberg A, Schrappe M, Cornish J, Peters C, ALL-BFM Study Group, et al. Allogeneic hematopoietic SCT in children with ALL: current concepts of ongoing prospective SCT trials. Bone Marrow Transplant 2008;41(Supplement 2):S71–4.
22. Bader P, Kreyenberg H, Henze GH, Eckert C, Reising M, Willasch A, et al. Prognostic value of minimal residual disease quantification before allogeneic stem-cell transplantation in relapsed childhood acute lymphoblastic leukemia: the ALL-REZ BFM Study Group. J Clin Oncol 2009;27:377–84.
23. Pulsipher MA, Langholz B, Wall DA, Schultz KR, Bunin N, Carroll WL, et al. The addition of sirolimus to tacrolimus/methotrexate GVHD prophylaxis in children with ALL: a phase 3 Children's Oncology Group/Pediatric Blood and Marrow Transplant Consortium trial. Blood 2014;123:2017–25.
24. Bader P, Kreyenberg H, von Stackelberg A, Eckert C, Salzmann-Manrique E, Meisel R, et al. Monitoring of minimal residual disease after allogeneic stem-cell transplantation in relapsed childhood acute lymphoblastic leukemia allows for the identification of impending relapse: results of the ALL-BFM-SCT 2003 trial. J Clin Oncol 2015;33:1275–84.
25. Dourthe ME, Rabian F, Yakouben K, Chevillon F, Cabannes-Hamy A, Mechinaud F, et al. Determinants of CD19-positive vs CD19-negative relapse after tisagenlecleucel for B-cell acute lymphoblastic leukemia. Leukemia 2021 May 17 [Epub ahead of print].
26. Ching T, Duncan ME, Newman-Eerkes T, McWhorter MME, Tracy JM, Steen MS, et al. Analytical evaluation of the clonoSEQ Assay for establishing measurable (minimal) residual disease in acute lymphoblastic leukemia, chronic lymphocytic leukemia, and multiple myeloma. BMC Cancer 2020;20:612.
27. Grupp SA, Kalos M, Barrett D, Aplenc R, Porter DL, Rheingold SR, et al. Chimeric antigen receptor-modified T cells for acute lymphoid leukemia. N Engl J Med 2013;368:1509–18.

AACR American Association for Cancer Research

BLOOD CANCER DISCOVERY

Next-Generation Sequencing of Minimal Residual Disease for Predicting Relapse after Tisagenlecleucel in Children and Young Adults with Acute Lymphoblastic Leukemia

Michael A. Pulsipher, Xia Han, Shannon L. Maude, et al.

Blood Cancer Discov 2022;3:66-81. Published OnlineFirst December 1, 2021.

Updated version	Access the most recent version of this article at: doi: 10.1158/2643-3230.BCD-21-0095
Supplementary Material	Access the most recent supplemental material at: http://bloodcancerdiscov.aacrjournals.org/content/suppl/2021/11/11/2643-3230.BCD-21-0095.DC1

Cited articles	This article cites 25 articles, 14 of which you can access for free at: http://bloodcancerdiscov.aacrjournals.org/content/3/1/66.full#ref-list-1

E-mail alerts	Sign up to receive free email-alerts related to this article or journal.
Reprints and Subscriptions	To order reprints of this article or to subscribe to the journal, contact the AACR Publications Department at pubs@aacr.org.
Permissions	To request permission to re-use all or part of this article, use this link http://bloodcancerdiscov.aacrjournals.org/content/3/1/66. Click on "Request Permissions" which will take you to the Copyright Clearance Center's (CCC) Rightslink site.